

# Targeted Antithrombotic Protein Micelles

Wookhyun Kim, Carolyn Haller, Erbin Dai, Xiwei Wang, Christoph E. Hagemeyer, David R. Liu, Karlheinz Peter, and Elliot L. Chaikof\*

**Abstract:** Activated platelets provide a promising target for imaging inflammatory and thrombotic events along with site-specific delivery of a variety of therapeutic agents. Multifunctional protein micelles bearing targeting and therapeutic proteins were now obtained by one-pot transpeptidation using an evolved sortase A. Conjugation to the corona of a single-chain antibody (scFv), which binds to the ligand-induced binding site (LIBS) of activated GPIIb/IIIa receptors, enabled the efficient detection of thrombi. The inhibition of thrombus formation was subsequently accomplished by incorporating the catalytically active domain of thrombomodulin (TM) onto the micelle corona for the local generation of activated protein C, which inhibits the formation of thrombin. An effective strategy has been developed for the preparation of protein micelles that can be targeted to sites of activated platelets with broad potential for treatment of acute thrombotic events.

**P**latelets play a critical role in mediating thrombus formation, and accumulating evidence shows the participation of platelets in a wide range of inflammatory processes, which contribute to the development of atherosclerosis, cerebrovascular disease, rheumatoid arthritis, as well as inflammatory bowel disease, tumor growth, and metastasis. Characteristically, the release of ADP, thrombin, thromboxane, and other proinflammatory factors at the sites of acute or chronic inflammation, regardless of etiology, can lead to the activation of platelets and endothelial cells (ECs) with further recruitment of circulating platelets and inflammatory cells.<sup>[1]</sup> Considering the ubiquitous involvement of platelets in thrombosis and inflammation, a strategy targeting activated platelets provides a very attractive approach for the selective

delivery of antithrombotic and anti-inflammatory agents. In particular, the glycoprotein IIb/IIIa (GPIIb/IIIa) undergoes a conformational change at the time of platelet activation and, thereby, through the exposure of unique epitopes serves as a distinctive structural feature for selective targeting of activated platelets.<sup>[2]</sup>

Polymeric micelles are self-assembled nanoparticles with a core-shell structure and have recently emerged as a powerful therapeutic platform to detect and treat various diseases, especially cancer.<sup>[3]</sup> Advantages of polymeric micelles include their increased circulating half-life, high drug-loading capacity, and their ability to present multiple ligands for improved site-specific targeting. In this regard, block polypeptides, and in particular recombinant elastin-based protein polymers, represent a class of polymeric micelles that consist of chemically and conformationally distinct protein blocks self-assembled into a variety of structures.<sup>[4]</sup> Elastin-like polypeptide (ELP) protein micelles have several advantages over synthetic polymeric micelles in that they are highly monodisperse, biocompatible, and biodegradable.<sup>[5]</sup> In addition, the modular structure of ELP micelles is easily tailored and functionalized using either chemical or enzymatic methods. Diblock polypeptides fused to small proteins have afforded multivalent ELP micelles displaying proteins at the corona by temperature-mediated self-assembly.<sup>[6]</sup> Tumor targeting has been pursued by genetically fusing RGD and NGR motifs to the hydrophilic portion of diblock ELPs.<sup>[7]</sup>


Herein, we describe the efficient and rapid formulation of multivalent, multifunctional protein micelles by one-pot transpeptidation using an evolved sortase A. Targeted delivery to activated platelets was achieved using a single-chain antibody that selectively binds to the ligand-induced binding site (LIBS) of activated GPIIb/IIIa receptors (anti-LIBS scFv).<sup>[8]</sup> In turn, thrombin generation was inhibited by incorporation of the catalytically active domain of thrombomodulin onto the micelle corona. Thrombomodulin alters the substrate specificity of thrombin, such that it preferentially activates protein C, which subsequently inactivates coagulation factors Va and VIIIa, thereby limiting further thrombin formation.<sup>[9]</sup> The effectiveness of this strategy in limiting thrombus growth and propagation in vivo demonstrates the therapeutic potential of multifunctional protein micelles.

Although protein fusion can be readily achieved using recombinant DNA techniques, bacterial expression of a fusion construct may be limited by low yield, loss of protein activity as a result of protein misfolding, and the formation of inclusion bodies that require a refolding process.<sup>[10]</sup> As an alternative, chemical or enzymatic schemes can be used to mediate the conjugation between reactive functional groups or appropriate peptide substrates. In this study, sortase-mediated bioconjugation was employed<sup>[8a,b,11]</sup> to attach

[\*] Dr. W. Kim, Dr. C. Haller, Dr. E. Dai, Prof. E. L. Chaikof  
Department of Surgery, Beth Israel Deaconess Medical Center  
Harvard Medical School  
110 Francis St, Suite 9F, Boston, MA 02115 (USA)  
and  
the Wyss Institute of Biologically Inspired Engineering of  
Harvard University  
Boston, MA (USA)  
E-mail: echaikof@bidmc.harvard.edu

X. Wang, Dr. C. E. Hagemeyer, Prof. K. Peter  
Atherothrombosis and Vascular Biology, Baker IDI Heart and  
Diabetes Institute  
PO Box 6492, St Kilda Rd Central, Victoria 8008 (Australia)

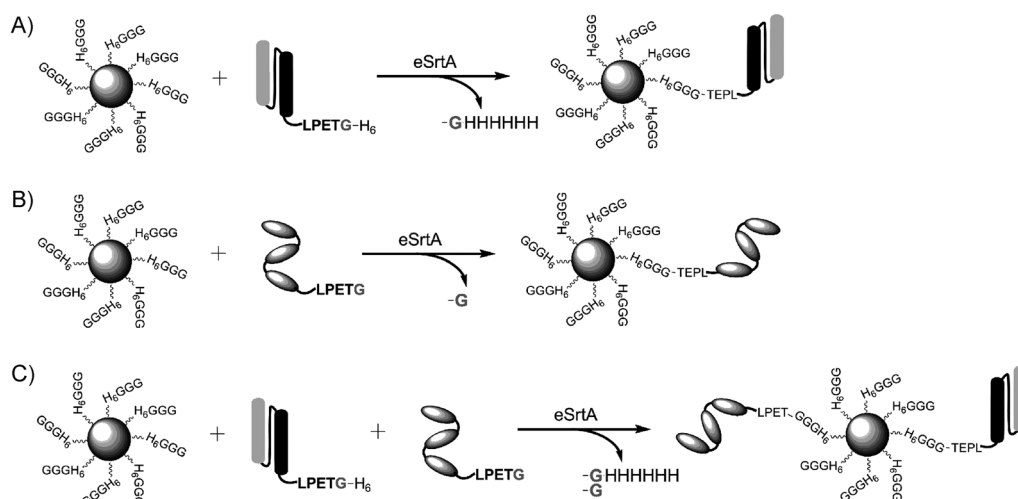
Prof. D. R. Liu  
Howard Hughes Medical Institute, Department of Chemistry and  
Chemical Biology, Harvard University  
Cambridge, MA 02138 (USA)

 Supporting information for this article is available on the WWW  
under <http://dx.doi.org/10.1002/anie.201408529>.

a single-chain antibody and a recombinant, catalytically active construct of thrombomodulin through C-terminal LPETG motifs to protein micelles that bear an N-terminal triglycine (GGG) oligopeptide. An amphiphilic diblock elastin-mimetic polypeptide was used to form spherical micelles ( $d \approx 50$  nm), which self-assembled through a temperature-driven conformational change of the hydrophobic block.<sup>[4a]</sup> Diblocks were generated with a nucleophilic triglycine motif followed by a His tag that was genetically incorporated at the N-terminal end of the hydrophilic block. The recombinant single-chain antibody selectively binds to activated GPIIb/IIIa receptors and was re-engineered with a C-terminal LPETG-His6 peptide motif. A human TM fragment containing the catalytically active EGF-like 456 domains was also expressed with a C-terminal LPETG motif (TM-LPETG), as well as an N-terminal FLAG tag, which facilitated the purification using anti-

FLAG affinity chromatography.<sup>[12]</sup> An evolved sortase A pentamutant (eSrtA), previously generated by directed evolution,<sup>[13]</sup> was used to conjugate scFv, TM or both scFv and TM to the N-terminal GGG motif of the micelle corona so as to produce a set of multifunctional micelles (Scheme 1).

Protein conjugation to ELP micelles using eSrtA was first investigated by SDS-PAGE gel electrophoresis (Figure 1). Micelles were initially produced from an aqueous solution of GGG-diblock copolymer ( $8 \mu\text{M}$ ) and then used in all reactions



**Scheme 1.** Preparation of multivalent, multifunctional protein micelles using sortase A. A) scFv-micelle, B) TM-micelle, and C) scFv/TM-micelle.

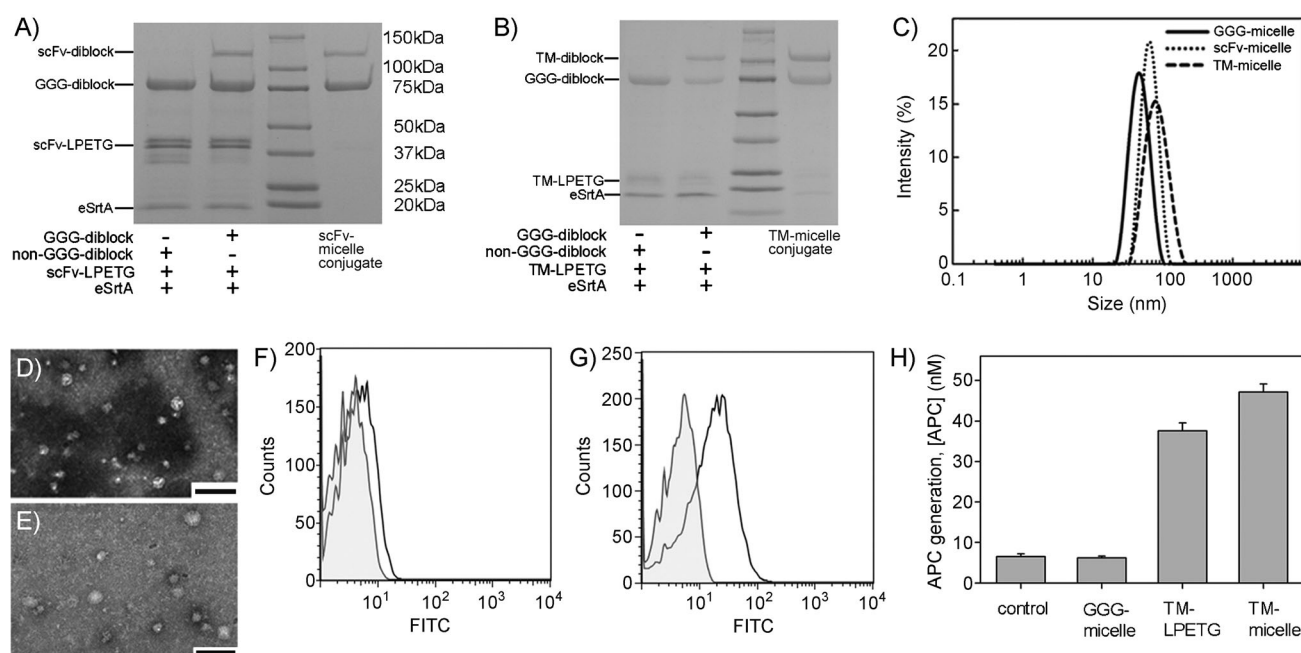


**Figure 1.** Characterization of protein micelles derivatized with either anti-LIBS-scFv or TM. SDS-PAGE gels showing conjugation of A) scFv and B) TM to protein micelles using sortase. Functionalization of GGG-micelles with therapeutic proteins demonstrates substrate specificity toward the GGG-diblock rather than non-GGG-diblock protein polymers. C) DLS measurements of GGG-micelles (solid), scFv-micelles (dot), and TM-micelles (dash). TEM images of D) scFv-micelles and E) TM-micelles (scale bars: 100 nm). Flow cytometry demonstrates the inability of GGG-micelles (F), but not scFv-micelles (G) to bind to activated (white curve) but not resting (gray curve) platelets. H) In vitro aPC generation by TM-micelles and an equivalent amount of TM-LPETG, as a positive control. TM activity was retained after micelle conjugation. GGG-micelles and saline (without TM or GGG-micelles) were used as negative controls ( $n = 3$ ).

at a final concentration of 4  $\mu\text{M}$  (CMC 3.5  $\mu\text{M}$ ). Micelles were incubated with LPETG-tagged scFv and eSrtA (1  $\mu\text{M}$ ) in a buffered solution (50 mM Tris-HCl, 150 mM NaCl, 0.5 mM  $\text{CaCl}_2$ , pH 7.5) at room temperature. Conjugation of scFv to the protein diblock afforded a scFv-LPETG-GGG-diblock, as evident by a new band, which was 30 kD higher than the original diblock with maximum yield achieved in 1 h (Figure 1A). Likewise, a TM-LPETG-GGG-diblock conjugate was successfully obtained (Figure 1B). A low ratio of sortase-to-substrate was used to minimize side reactions, including the formation of acyl-enzyme intermediates and hydrolysis-related side products. At a 1  $\mu\text{M}$  concentration of eSrtA, functionalization of micelles with scFv (scFv-micelle) and TM (TM-micelle) was observed after 1 h without side products. Reaction conditions were optimized for a maximum conjugation of micelles with scFv or TM (see the Supporting Information, Figure S2A,B). Incubation of GGG-micelle with scFv-LPETG (8 equiv to GGG-diblock) or TM-LPETG (3 equiv to GGG-diblock) afforded yields of approximately 15 and 50%, respectively, as quantified by SDS-PAGE gel analysis based on the ratio of GGG-diblock band intensity before and after conjugation. Diblock conjugates were not observed in the absence of eSrtA or in the presence of micelles that did not contain N-terminal GGG motifs (Figure 1A,B). Significant differences in the conjugation of scFv or TM was attributed to steric hindrance as a result of differences in protein size with less accessibility to the C-terminal LPETG motif of the scFv. Purification was achieved by size-exclusion centrifugal filtration (MWCO 100 kDa) to remove unreacted LPETG-tagged scFv or TM and eSrtA.

Dynamic light scattering (DLS) and transmission electron microscopy (TEM) were used to characterize the conjugation of micelles (Figure 1C–E). Average diameters of scFv and TM micelles were 61 and 77 nm, respectively, which was larger than that of the initial GGG-micelle (50 nm), consistent with reports for TM-functionalized liposomes<sup>[14]</sup> and other protein-functionalized ELP micelles.<sup>[6a,15]</sup> TEM demonstrated the formation of uniform spheres of 30 to 40 nm in diameter, consistent with the imaging of micelles in a dehydrated state. The zeta potential of GGG-micelles, which contains glutamic acid residues in the outer shell was negative (−13 mV).<sup>[4c,15]</sup> After conjugation with scFv or TM, the zeta potential at neutral pH value decreased to −18 and −16 mV, respectively.

Binding of scFv-micelles to activated platelets was assessed by flow cytometry (Figure 1F,G). As anticipated, scFv-micelles did not bind to resting, non-activated platelets, but bound selectively to activated platelets, which was not observed for GGG-micelles. TM-micelle conjugation enhanced the production of activated protein C (aPC), comparable to the effect of free TM-LPETG (Figure 1H). aPC was not generated by GGG-micelle in the absence of TM. These data indicate that scFv and TM remain fully active after conjugation to the hydrophilic shell of protein micelles.

Binding of micelles to platelet-rich thrombi was examined by intravital microscopy using a murine cremaster muscle microcirculation model in which thrombi were formed by laser-induced vascular injury. GGG- and scFv-targeted micelles containing N-terminal His tags were pre-incubated

with Alexa Fluor 488 conjugated to an antipenta His antibody. Intravital microscopy demonstrated specific binding of targeted micelles to platelet-rich thrombi, whereas GGG-micelles displayed no detectable background binding (Figure 2).

The generation of multifunctional micelles requires the reliable introduction of multiple functional components.<sup>[3,16]</sup> Peters and colleagues developed micelles that contained an

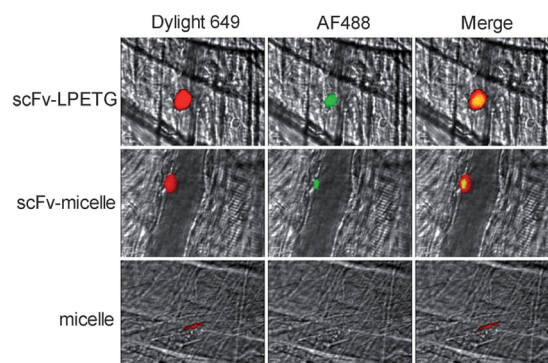


**Figure 2.** scFv-micelles target to platelet thrombus in vivo. Platelet-specific Dylight 649-labeled anti-CD42b was infused along with either AF488-labeled scFv-LPETG (top row), AF488-labeled scFv-micelles (middle row), or AF488-labeled micelles (bottom row) prior to laser injury of cremaster arterioles. Representative images illustrate that scFv-LPETG (top row) and scFv-micelles (middle row) target to platelet thrombus. Co-localization of nonfunctionalized GGG-micelles to platelet thrombi was not observed (bottom row).

oligopeptide clot-binding element, a fluorophore, and hirulog, which targeted fibrin deposited on atherosclerotic plaques.<sup>[3]</sup> Likewise, PEG-lipid micelles have been functionalized with a fibrin-targeting peptide (CREKA), a fluorescent dye, and hirulog, for targeted delivery of an anticoagulant to sites of atherosclerosis. The tethering of two or more constituents to nano- or microparticles, as well as DNA scaffolds has been achieved by physioadsorption, biotin–streptavidin binding interactions or chemical coupling techniques with applications in biosensors, cofactor recycling, or biocatalytic cascades for the synthesis of biological materials.<sup>[17]</sup> Although such approaches are relatively straightforward, nonorthogonal bioconjugation often leads to inactivation of a critical active site or protein misorientation, leading to loss of protein activity. In this study, anti-LIBS scFv facilitated selective micelle binding to activated GPIIb/IIIa receptors, while TM enhanced thrombin-mediated aPC generation. Micelles were functionalized with both LPETG-tagged proteins using a one-pot sortase reaction (Scheme 1C). Briefly, GGG-micelles were incubated with anti-LIBS scFv-LPETG and TM-LPETG in the presence of eSrtA (1 h incubation, 4  $\mu\text{M}$  GGG-diblock, 30  $\mu\text{M}$  scFv-LPETG, 12  $\mu\text{M}$  TM-LPETG, 1  $\mu\text{M}$  eSrtA). Conjugation of scFv and TM to protein micelles produced two new bands on SDS PAGE gels corresponding to the scFv-LPETG-GGG-diblock and TM-LPETG-GGG-diblock (Figure 3A). Optimized reaction conditions allowed co-functionalization to GGG-diblocks within a 1 h period using 8 equiv of scFv-LPETG and 3 equiv of TM-LPETG (Sup-



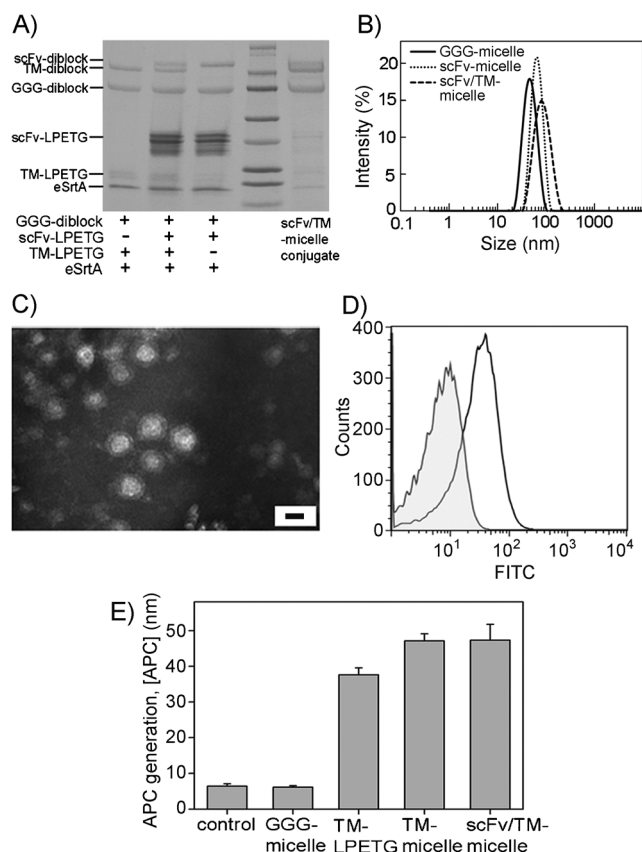


**Figure 3.** Characterization of protein micelles derivatized with both anti-LIBS-scFv and TM. A) SDS-PAGE gels demonstrating conjugation of scFv and TM to protein micelles using an evolved sortase. B) DLS measurements of GGG-micelles (solid line), scFv-micelles (dotted line) and scFv/TM-micelles (dashed line). C) TEM images of scFv/TM-micelles (scale bar: 20 nm). D) Flow cytometry assay demonstrating successful conjugation of scFv to protein micelles with specific binding of scFv/TM-micelles to activated (white curve) but not resting platelets (gray curve). E) In vitro aPC generation by scFv/TM-micelles. TM activity was retained after cofunctionalization of micelles with both scFv and TM. GGG-micelles and saline (without TM and GGG-micelle) were used as negative controls ( $n = 3$ ).

porting Information, Figure S2). Cofunctionalization of micelles was confirmed by selective fluorescent labeling of TM, which afforded a single fluorescent band corresponding to the TM-LPET-GGG-diblock. The amount of conjugated TM was quantified by in-gel fluorescence scanning. Approximately 50% of the GGG-diblock was conjugated to TM ( $\approx 10 \mu\text{g}$  of TM/ $100 \mu\text{g}$  of protein micelles; Supporting Information, Figures S3 and S4).

The average diameter and zeta potential of bifunctional scFv/TM-micelles (targeted TM micelle) were 75 nm and  $-14 \text{ mV}$ , respectively (Figure 3B,C). TEM of dehydrated samples confirmed that these micelles were uniform spheres of 30 to 40 nm in diameter. Targeted TM micelles demonstrated specific binding to activated platelets by flow cytometry along with enhanced aPC generation, which was not observed using nonderivatized GGG-micelles (Figure 3D,E). These results confirm that co-immobilization of scFv and TM afforded multivalent, multifunctional micelles that selectively bind to activated platelets with local generation of aPC.

The approach described in this manuscript is motivated by the idea that clinical efficacy of antithrombotic therapy can be significantly improved through targeted delivery to sites of injury. The chosen targeting strategy is based upon the principle that activated platelets serve as an ideal epitope for the delivery of agents targeted to the site of vascular wall injury, given their early and spatial involvement in coagulation. To this end, we report the site-specific modification of protein micelles with both a scFv targeting handle to activated platelets and an antithrombotic therapeutic handle. Through in vitro assays, we confirmed that both scFv and TM retain their individual function after conjugation to micelles. To examine the therapeutic significance of our targeting approach in vivo, we employed a well-established model of laser-injury-induced arteriole thrombosis.<sup>[18]</sup> Intravital video-microscopy allows real-time monitoring of platelet accumulation, as well as visualization of targeted micelles co-localizing with activated platelets. Significantly, only those micelles that contained the scFv targeting group enriched thrombi (Figure 2) and inhibition of thrombus formation only occurred after administration of micelles bearing both scFv and TM (Figure 4). When an equimolar dose of nontargeted TM-micelles was infused, thrombus formation was not affected. Thus, therapeutic targeting presents a promising approach to reduce the magnitude of the antithrombotic agent often required to achieve a clinically meaningful effect following systemic delivery.

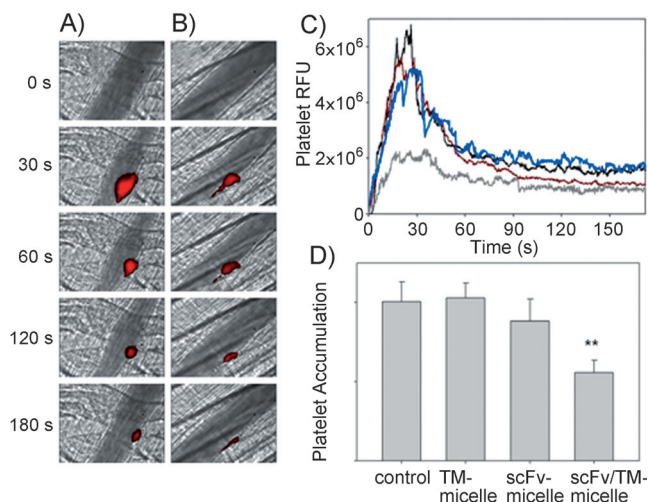


**Figure 4.** TM-micelles targeted to activated platelets inhibit thrombus formation in vivo. Platelet-specific anti-CD42b-Dylight 649 was infused and laser-injury-induced thrombus formation was characterized over time. Representative images of the fluorescence signal associated with a platelet thrombus after laser injury of cremaster arterioles are administration of A) saline or B) scFv/TM-micelles (0.026  $\mu\text{mol}$  TM/kg). C) Median integrated platelet fluorescence after administration of saline (black), TM-micelles (0.026  $\mu\text{mol}$  TM/kg; blue), scFv-micelles (red), or scFv/TM-micelles (grey). D) Platelet accumulation was quantified as the area under the curve (AUC) as calculated for platelet RFU. Units are arbitrary and data represent mean  $\pm$  SEM. A significant reduction in platelet accumulation was observed in those animals treated with scFv/TM-micelles ( $N = 25$  thrombi/3 mice/group, \*\* $p < 0.01$ ).

In conclusion, we have developed multivalent, multifunctional protein micelles, functionalized with both an scFv that is specific to activated GPIIb/IIIa receptors and a human TM fragment using sortase-mediated bioconjugation. In comparison with previously reported studies that genetically fused small proteins (< 20 kDa) and peptides (3–20 amino acids) to micelle-forming ELP diblock polypeptides,<sup>[6a,7a,15]</sup> selective covalent conjugation of multiple relatively large proteins ( $\approx$  40 kDa) was achieved without the loss of bioactivity. Chemoenzymatic bio-orthogonal conjugation provides a highly efficient strategy for cofunctionalization of diverse molecules onto micelles or other nanoparticle carriers. In this study, multifunctional protein micelles displayed a high level of site-specific targeting to thrombi with local generation of an inhibitor of the coagulation cascade. These results prove the feasibility of targeted delivery of a potent antithrombotic to sites of platelet thrombi, which will likely facilitate a reduction in anticoagulant dose and bleeding risk.

Received: August 25, 2014

Revised: October 9, 2014

Published online: December 10, 2014

**Keywords:** bioconjugation · drug delivery · micelles · therapeutic proteins · thrombosis

- [1] N. Mackman, *Nature* **2008**, *451*, 914–918.
- [2] D. Cox, M. Brennan, N. Moran, *Nat. Rev. Drug Discovery* **2010**, *9*, 804–820.
- [3] D. Peters, M. Kastantin, V. R. Kotamraju, P. P. Karmali, K. Gujraty, M. Tirrell, E. Ruoslahti, *Proc. Natl. Acad. Sci. USA* **2009**, *106*, 9815–9819.
- [4] a) W. Kim, J. Thevenot, E. Ibarboure, S. Lecommandoux, E. L. Chaikof, *Angew. Chem. Int. Ed.* **2010**, *49*, 4257–4260; *Angew. Chem.* **2010**, *122*, 4353–4356; b) W. Kim, J. Xiao, E. L. Chaikof, *Langmuir* **2011**, *27*, 14329–14334; c) W. Kim, C. Brady, E. L. Chaikof, *Acta Biomater.* **2012**, *8*, 2476–2482.
- [5] a) S. R. Ong, K. A. Trabbic-Carlson, D. L. Nettles, D. W. Lim, A. Chilkoti, L. A. Setton, *Biomaterials* **2006**, *27*, 1930–1935; b) M. Shah, P. Y. Hsueh, G. Sun, H. Y. Chang, S. M. Janib, J. A. MacKay, *Protein Sci.* **2012**, *21*, 743–750.
- [6] a) W. Hassounah, K. Fischer, S. R. MacEwan, R. Branscheid, C. L. Fu, R. Liu, M. Schmidt, A. Chilkoti, *Biomacromolecules* **2012**, *13*, 1598–1605; b) P. Shi, S. Aluri, Y. A. Lin, M. Shah, M. Edman, J. Dhandhukia, H. Cui, J. A. MacKay, *J. Controlled Release* **2013**, *171*, 330–338; c) G. Sun, P. Y. Hsueh, S. M. Janib, S. Hamm-Alvarez, J. A. MacKay, *J. Controlled Release* **2011**, *155*, 218–226.
- [7] a) A. J. Simnick, M. Amiram, W. Liu, G. Hanna, M. W. Dewhirst, C. D. Kontos, A. Chilkoti, *J. Controlled Release* **2011**, *155*, 144–151; b) A. J. Simnick, C. A. Valencia, R. Liu, A. Chilkoti, *ACS Nano* **2010**, *4*, 2217–2227.
- [8] a) M. K. Leung, C. E. Hagemeyer, A. P. Johnston, C. Gonzales, M. M. Kamphuis, K. Ardipradja, G. K. Such, K. Peter, F. Caruso, *Angew. Chem. Int. Ed.* **2012**, *51*, 7132–7136; *Angew. Chem.* **2012**, *124*, 7244–7248; b) H. T. Ta, S. Prabhu, E. Leitner, F. Jia, D. von Elverfeldt, K. E. Jackson, T. Heidt, A. K. Nair, H. Pearce, C. von Zur Muhlen, X. Wang, K. Peter, C. E. Hagemeyer, *Circ. Res.* **2011**, *109*, 365–373; c) M. Schwarz, G. Meade, P. Stoll, J. Ylanne, N. Bassler, Y. C. Chen, C. E. Hagemeyer, I. Ahrens, N. Moran, D. Kenny, D. Fitzgerald, C. Bode, K. Peter, *Circ. Res.* **2006**, *99*, 25–33.
- [9] C. T. Esmon, *FASEB J.* **1995**, *9*, 946–955.
- [10] D. Topcic, W. Kim, J. K. Holien, F. Jia, P. C. Armstrong, J. D. Hohmann, A. Straub, G. Krippner, C. A. Haller, H. Domeij, C. E. Hagemeyer, M. W. Parker, E. L. Chaikof, K. Peter, *Arterioscler. Thromb. Vasc. Biol.* **2011**, *31*, 2015–2023.
- [11] M. W. Popp, J. M. Antos, G. M. Grotenbreg, E. Spooner, H. L. Ploegh, *Nat. Chem. Biol.* **2007**, *3*, 707–708.
- [12] C. S. Cazalis, C. A. Haller, L. Sease-Cargo, E. L. Chaikof, *Bioconjugate Chem.* **2004**, *15*, 1005–1009.
- [13] I. Chen, B. M. Dorr, D. R. Liu, *Proc. Natl. Acad. Sci. USA* **2011**, *108*, 11399–11404.
- [14] H. Zhang, J. Weingart, R. Jiang, J. Peng, Q. Wu, X. L. Sun, *Bioconjugate Chem.* **2013**, *24*, 550–559.
- [15] C. García-Arévalo, J. F. Bermejo-Martin, L. Rico, V. Iglesias, L. Martin, J. C. Rodríguez-Cabello, F. J. Arias, *Mol. Pharm.* **2013**, *10*, 586–597.
- [16] V. M. Y. Yurko, E. Andreozzi, G. L. Thompson, A. A. Vertegel, *Mater. Sci. Eng. C* **2009**, *29*, 737–741.
- [17] a) E. J. Cho, S. Jung, H. J. Kim, Y. G. Lee, K. C. Nam, H. J. Lee, H. J. Bae, *Chem. Commun.* **2012**, *48*, 886–888; b) T. Matsumoto, T. Tanaka, A. Kondo, *Langmuir* **2012**, *28*, 3553–3557; c) L. Betancor, C. Berne, H. R. Luckarift, J. C. Spain, *Chem. Commun.* **2006**, 3640–3642; d) O. I. Wilner, Y. Weizmann, R. Gill, O. Lioubashevski, R. Freeman, I. Willner, *Nat. Nanotechnol.* **2009**, *4*, 249–254.
- [18] R. Jasuja, F. H. Passam, D. R. Kennedy, S. H. Kim, L. van Hessem, L. Lin, S. R. Bowley, S. S. Joshi, J. R. Dilks, B. Furie, B. C. Furie, R. Flaumenhaft, *J. Clin. Invest.* **2012**, *122*, 2104–2113.